Qualitative and Quantitative Recognition of Volatile Organic Compounds in Their Liquid Phase Based on Terahertz Microfluidic EIT Meta-Sensors

Wenfeng Fu, Li Sun, Hongyan Cao, Lin Chen, *Member, IEEE*, Ming Zhou, Shengyuan Shen, Yiming Zhu, *Senior Member, IEEE*, and Songlin Zhuang

***Abstract*—Volatile organic compounds (VOCs) are directly associated with human health concerns and environmental safety. Therefore, it is urgent to achieve accurate detection of VOCs both qualitatively and quantitatively. In this work, the qualitative detection of ethyl benzene (EB), isopropyl alcohol (IPA), and ethyl acetate (EA)—three pure VOCs in liquid phase—was discussed using terahertz (THz) microfluidic electromagnetic-induced transparency (EIT) meta-sensors. The THz response illustrated that with an increase in VOCs' volumes (1–6 μL), resonant frequencies of dual transmission dips (0.855 and 1.724 THz) and the EIT peak (1.213 THz) exhibited redshift. The limit of detections (LODs) for pure IPA, EA, and EB can achieve 5.45, 13.46, and 4.35 μg, respectively. The multivariate fusion (MF) model based on the EIT responses to VOCs was utilized to improve the accuracy of trace detection and classification of VOCs. Furthermore, the above method combined with principal component analysis with the Gaussian mixture model (PCA-GMM) and the neural network classification algorithm support vector machine (SVM) was applied to the recognition of VOCs. In addition, the THz method is not feasible to detect trace amounts of VOCs (typically 0.3 mg/L) in wastewater because water is highly absorbable in the THz band and VOCs will evaporate if water is removed. Here, IPA, EA, and EB in soil were detected and classified by PCA-GMM combined with MF. Our results provide a new THz meta-sensor platform to trace the detection of VOCs in the liquid phase and soil and may be used to identify hazardous wastes in illegal dumping.**

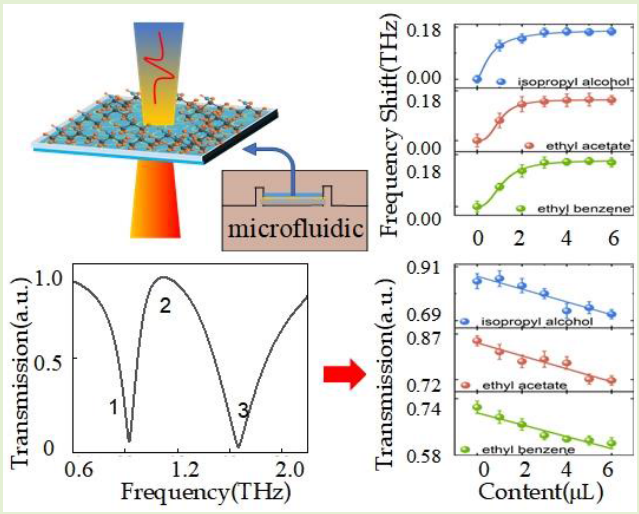

***Index Terms*— Electromagnetic-induced transparency (EIT), microfluidics, terahertz (THz), volatile organic compounds (VOCs).**

I. Introduction

VOLATILE organic compounds (VOCs) refer to the special type of organic compounds under normal conditions. As varieties of industries have developed and evolved, VOCs are typical byproducts generated from industrial processes (including the petroleum industry, chemical industry, industrial painting, and coal-coking industry). VOCs do serious harm to human health and environmental safety even if at reasonably low concentrations. VOCs can be divided into hydrocarbons and aerobic organic compounds both in gas and liquid phases [1], [2], [3]. VOCs are common to see including benzene, ethyl acetate (EA), isopropyl alcohol (IPA), ethyl benzene (EB), toluene, and so on [4]. VOCs can be divided into alcohols, aromatic compounds, aldehydes, and ketones based on their functional groups, and most of them are toxic. VOCs bring adverse effects on the human body system (e.g., circulatory, nervous, reproductive, cardiovascular, immune, and respiratory systems) and special organs (e.g., kidneys, liver, stomach, and spleen) [4]. For VOCs in the liquid phase, conventional detection methods are liquid

Manuscript received 6 March 2023; revised 14 April 2023; accepted 14 April 2023. Date of publication 21 April 2023; date of current version 14 June 2023. This work was supported in part by the Basic Science Center Project of the National Natural Science Foundation of China under Grant 61988102; in part by the National Natural Science Foundation of China under Grant 62275157; in part by the Shanghai Shuguang Program, China, under Grant 18SG44; in part by the 111 Project under Grant D18014. The associate editor coordinating the review of this article and approving it for publication was Prof. Santosh Kumar. *(Wenfeng Fu, Li Sun, and Hongyan Cao contributed equally to this work.) (Corresponding author: Lin Chen.)*

Please see the Acknowledgment section of this article for the author affiliations.

This article has supplementary downloadable material available at https://doi.org/10.1109/JSEN.2023.3268167, provided by the authors.

Digital Object Identifier 10.1109/JSEN.2023.3268167

chromatography (LC) [5] and Fourier transform infrared spectroscopy (FTIR) [6]. The former is limited by professional technicians, off-site analysis, and matrix-matching calibration criteria. And the latter as the optical method has elevated demand for the laboratory detection environment and a lower signal-to-noise ratio. Otherwise, both the aforementioned methods are time-consuming, costly, and inconvenient, which means that they are not available for fast field detection of VOCs. More recently, at optical and infrared frequencies, photonic crystal fiber-based surface plasmon resonance sensors were also widely used for the detection of physical and biochemical parameters. Their potential application for the detection of VOCs in the liquid phase can still need to be explored [7], [8], [9], [10], [11]. Therefore, a fast and useful device for the detection and identification of rarely destructive VOCs is urgently needed. Terahertz (THz) detection has the advantages of nondestructive, high speed, and low energy consumption [12], [13]. It has been widely used in food [14], chemistry [15], biology [16], imaging [17], communication [18], and other fields. For the detection and chemical identification of such increased VOC contaminants, THz spectroscopic detection is considered a new and complementary method to conventional analytical approaches and a hopeful technique to distinguish differences from materials in solid or liquid phases [19], [20]. Some research studies on VOC detection have been extensively studied in the THz band. For example, Barnes et al. [21] used THz time-domain spectroscopy (THz-TDS) to study the absorption coefficient and refractive index of liquid benzene from 2.1 to 7.5 THz. Ronne et al. [22] also successfully distinguished liquid toluene from benzene with THz spectroscopy. In addition, three temperature-dependent benzene isomers were selected to observe their intermolecular dynamics. The identification of gasoline, kerosene, and toluene in the liquid phase was also achieved by analyzing their transmittance and refractive index from 0.3 to 1.8 THz [23]. Annalisa et al. [19] did similar research on measuring the refractive index and absorption coefficient from 0.2 to 2.5 THz to discriminate specific VOCs (benzene, styrene, toluene, and p-xylene) in the liquid phase. However, the thickness of the cell is so thick that it does not match the trace detection in a real application (e.g., 5 mm in [19]). Since then, plenty of research still need to be contributed to the trace detection of VOCs in the THz domain.

In recent years, meta-sensors have received a lot of attention to gain new detection approaches. Meta-sensors, composed of artificial unit cells, have remarkable resonant properties beyond natural materials [24], [25], [26], [27], [28]. The dielectric properties of the measured analyte will affect the resonant electrical signal of the meta-sensor. Such resonant signals commonly include resonant frequency shifts and amplitude variations. The frequency shift is caused by the strong light–matter interaction with the analyte, while the amplitude change is due to the electric field variable [29], [30]. Trace VOC detection as a practical application is easy to be disturbed by strong environmental factors, so it is difficult to accurately evaluate the performance only by a single aspect. It is not sufficient to analyze the THz resonance frequency shift and amplitude variation separately. To overcome the forward problem, a reflective THz multiband meta-sensor with synthetic evaluation criteria was used to achieve sensitive detection [31]. However, the reflection-type device requires

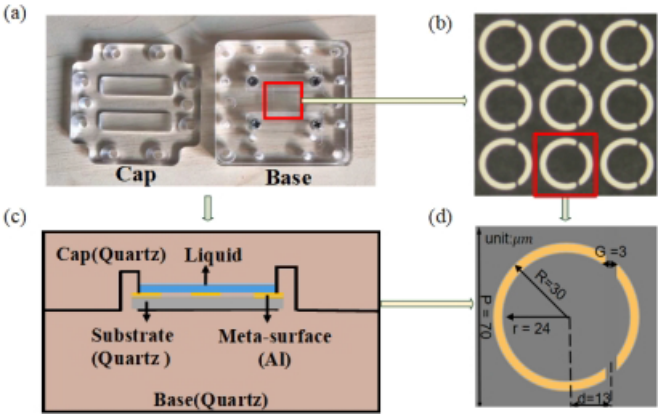

Fig. 1. (a) Photograph of the microfluidic sample cell assembled with the THz EIT meta-sensor. (b) Optical images of the EIT meta-sensor. (c) Schematic of the microfluidic chip. (d) Unit cell of the meta-sensor with key parameters.

oblique incidence due to the spatial overlap of illumination and collection in light paths. So, the transmissive version of the meta-sensor is preferred in practical applications [32], [33].

In this work, a meta-sensor structure based on electromagnetically induced transparency (EIT) [34], [35] which integrated with microfluidic was proposed for sensing and classification of three different VOCs: IPA, EA, and EB, in their liquid phase. The structure consists of two layers: the upper layer is an asymmetric split-ring resonator made of aluminum and the substrate is quartz with a permittivity of 3.75. The EIT analog appears in this particular configuration when the bright modes are suppressed and the quasi-dark modes are distributed by a strong electric field. Moreover, the completely enclosed microfluidic cell effectively prevents liquid volatilization. While monitoring the transmission spectrum with THz TDS, there was one resonant peak at 1.213 THz and two dips at 0.855 and 1.724 THz, which were used to study the characteristics of the meta-sensor when the pure liquid VOCs content varied (1–6 μL at intervals of 1 μL). We found that the resonant frequency shifts satisfied the Hill model and amplitudes satisfied linear fitting with reliable R_2 higher than 0.9. To evaluate the sensing performance of the EIT meta-sensor synthetically and identify VOCs efficiently, we proposed a multivariate fusion (MF) framework combined with principal component analysis with the Gaussian mixture model (PCA-GMM) and the neural classification algorithm support vector machine (SVM). Moreover, the VOCs-containing (1 μL) soil sample weighed 0.3 g which is approximately in line with the actual scenario was measured by the EIT meta-sensor with increased time. We found that the EIT resonance frequency shifts did not appear to be significant if the microscopic content of VOCs in the soil is evaporated. However, the amplitude of the EIT peak decreases linearly with time due to volatilization. The MF combined with PCA-GMM is useful for the classification of the three VOCs. When VOCs are in the soil, the limit of detection (LOD) is 2900 mg/kg [36] for EB. To our knowledge, it is the first time to achieve the monitoring of trace VOCs in soil by using THz meta-sensors, which have a great influence in distinguishing hazardous waste dumped without permission in soil quickly. Our results open a new THz meta-sensor perspective to realize the trace detection of VOCs in the liquid phase and soil.

II. THz EIT Meta-Sensor Integrated With Microfluidic

The construction of a microfluidic chip [37], [38], [39] is demonstrated in Fig. 1. Fig. 1(a) shows the photograph of a microfluidic sample cell assembled with the THz EIT meta-sensor. The left part is the quartz cap with 5 mm thickness, and the right part is the quartz base with 8 mm thickness. The schematic of the microfluidic setup in the x–z-direction is shown in Fig. 1(c). A series of fluids [such as IPA, EA, and EB provided by Shanghai Academy of Environmental Sciences, blue color in Fig. 1(c)] were detected by dripping them with a pipette onto the meta-sensor which was fixed on the quartz base and then covering the quartz cap. The purpose of inserting the cap into the base is to create a sealed space to prevent VOCs from volatilization for quantitative sensing of VOCs in their liquid phase. The meta-sensor consists of two parts: 1) a quartz substrate with a dielectric constant of 3.75 and a thickness of $h = 500$ μm; and 2) asymmetric crescent-shaped split-ring resonators (SRRs) with Al (conductivity of 3.56×10^7 S/m and the thickness of $t = 200$ nm). The optical image of the meta-sensor arrays is depicted in Fig. 1(b) by a microscope. The main dimension parameters of the unit cell in Fig. 1(d) are $P = 70$ μm, $R = 30$ μm, $r = 24$ μm, $G = 3$ μm, and the asymmetric parameter from the center of the gap to the ring center $d = 13$ μm. Advanced Testing Company 7500SU is used for experimental detection. To reach a relative humidity below 3% and eliminate the water vapor interference in the air, the sample bin of the equipment instrument was full of nitrogen before detection.

The simulated and measured transmission spectra of the EIT meta-sensors was shown in Fig. 2(a). The experimental results agree well with the simulation transmission spectra by CST Microwave Studio. Between two dips (0.855 THz marked by 1 and 1.724 THz marked by 2), a transmission peak (1.213 THz marked by 3) with an amplitude of 0.85 is shown in Fig. 2(a). The transparency window was believed to be evidence that it is the EIT effect [34]. The physical mechanism of the proposed meta-sensor is based on the EIT effect, which can be investigated by monitoring the electric field and the surface current of the two dips and the peak, as plotted in Fig. 2(b)–(g). At 0.855 THz (Position 1), an electric resonant mode of the left long arm was generated, as shown in the electric field in Fig. 2(b). The corresponding surface current distribution shown in Fig. 2(e) implies that the difference in the surface currents between the left long arm and right short arm demonstrates that this resonant mode is attributed to Fano resonance. Meanwhile, the asymmetric long and short circulating currents are formed along the two sides of the arms with an anticlockwise loop, which induces the weak magnetic field, as seen in Fig. 2(e). At 1.213 THz (Position 2), the electric field distribution transforms into the trapped mode in two gaps, which is nonradiative damping, as seen in Fig. 2(c). At the same time, the strong surface currents in the long and short arms form a closed clockwise loop, as found in Fig. 2(f) [40]. The out-phase magnetic fields are induced inside the metallic rings and the strength is enhanced, which results in the generation of magnetic dipole resonance. Here, the magnetic/electric dipole resonance from the short-length arm (dark mode) couples with the electric dipole from the long-length arm (bright mode), and the destructive interference leads to the suppression of the bright mode and couples the energy to the dark mode, thus the trapped mode is dominant. Under such conditions, the radiative losses are dramatically reduced, and the transmission window occurs accordingly. This can be verified in Fig. 2(a). At 1.724 THz (Position 3), the trapped mode transforms to the electric dipole mode, and the out-phase magnetic fields did not locate inside the metallic rings, as shown in Fig. 2(d) and (g). Here, the interference is reduced with the increase in frequency, and the radiative losses are dominant and the transmission window disappears. Such EIT spectra are featured by two dips and one transparent peak, whose resonant frequencies and intensities are sensitive to the surrounding environment, making EIT metasurface systems potential for sensor designs.

III. Neural Network SVM and PCA Based on MF Model Construction

The data analytical procedure to quantify and classify VOCs either in the pure liquid phase or in the soil is demonstrated in Fig. 3. The different VOCs are measured by THz-TDS with a meta-sensor. Then EIT resonant responses (frequency shifts and amplitude changes for three areas: two dips and one peak) are captured and fitted with an appropriate model to confirm if they show a high relative coefficient. Then, two widely used classification methods (neural network SVM and PCA-GMM algorithms) were used to construct different VOC quantification models and further classify them rapidly and accurately.

A. THz EIT Spectrum of Pure VOCs in Liquid

To quantitatively measure the trace VOCs (IPA, EA, and EB) in the six prepared samples (1–6 μL, intervals for 1 μL), different contents of VOCs were dripped on the surface of the meta-sensor and both spectral amplitude and frequency shift responses were analyzed. For accurate classification, we obtain transmission spectra by repeating measurements ten times for every content of single VOCs. The transmission spectra in Fig. 4(a), (c), and (e) show that the amplitude of the transmission peaks generally decreased but two dips increased; moreover, all three resonant frequency shifts decrease (redshift) with the increase of VOC volume. The frequency shift of transmission responses (positions 1–3) to the various VOC contents is depicted in Fig. 4(b), (d), and (f).

It can be seen that transmission frequency shift (positions 1–3) does not show a reliable linear relationship with increasing VOC contents, so the Hill fitting model [41] is chosen to describe their relationship instead. The Hill equation is given by

$$Fs = Fs_{\max} \times \frac{[\mathrm{VOC}]^n}{(K_D)^n + [\mathrm{VOC}]^n} \tag{1}$$

where F_S is the frequency shift, $Fs_{\max}$ is the maximum frequency shift, m is the VOC content, K_D is a constant, and n is the Hill coefficient. Table I lists nine Hill parameters for resonance frequencies at three positions with three VOCs. The R^2 is higher than 0.99. Fig. 4(b), (d), and (f) also depicts responses of the frequency shift to the increased VOC content, which means that all nine amplitudes showed linear

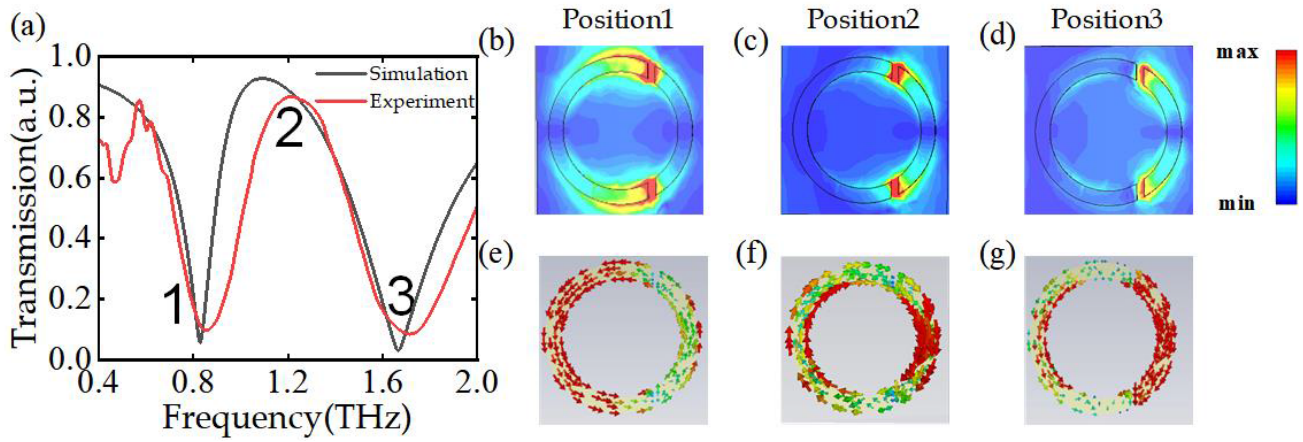

Fig. 2. (a) Simulated and experimental transmission spectra of the meta-surface. (b)–(g) Electric field and surface current at three frequency positions marked by 1–3 in (a), respectively.

TABLE I
FREQUENCY SHIFT RESPONSE WITH THE HILL FITTING MODEL AND AMPLITUDE RESPONSE WITH THE LINEAR MODEL

Peaks	VOCs	Hill fitting				Linear model		
		Fs_{max} (THz)	K_D	n	R^2	a	b	R^2
Position1	IPA	0.1181	0.6343	1.3237	0.997	0.025888	0.0877	0.903
	EA	0.1087	0.8877	2.4605	0.998	0.0241	0.1112	0.838
	EB	0.1469	0.5839	0.5117	0.997	0.0133	0.06615	0.949
Position2	IPA	0.1723	0.6339	1.46989	0.997	-0.0261	0.8707	0.922
	EA	0.1477	0.8879	2.9456	0.999	-0.0214	0.8408	0.941
	EB	0.1560	0.5898	2.4960	0.997	-0.0168	0.7997	0.894
Position3	IPA	0.1616	0.6335	1.70834	0.999	0.0201	0.0731	0.889
	EA	0.1175	0.8884	1.6344	0.997	0.0217	0.0771	0.8523
	EB	0.1902	0.5906	1.5170	0.999	0.0136	0.0564	0.964

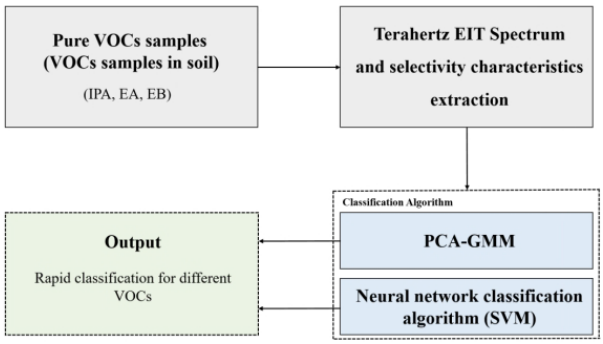

Fig. 3. Procedure to quantify and classify pure VOCs or VOCs in soil.

relationships with increased VOC content. The linear equation is given by

$$T = ax + b \tag{2}$$

where a is the slope, b is the intercept, and x is the amplitude. The R^2 for the amplitude of three VOCs in three positions is all higher than 0.8. Table I also lists nine linear parameters for resonance amplitudes at three positions in detail.

Then, the LOD of the VOC C_{lim} can be obtained by

$$C_{\text{lim}} = K_D \cdot \frac{1}{\Delta f_{\max}/S_f - 1} \tag{3}$$

where S_f is a spectral resolution of 1.9 GHz. The C_{lim} of IPA, EA, and EB is 0.007 μL (5.45 μg), 0.015 μL (13.46 μg), and 0.005 μL (4.35 μg), respectively. According to the frequency shifts and amplitudes obtained above, two classification methods were applied to trace the detection of different VOCs. We also simulated the transmission spectra of three VOCs with different volumes. The results are shown in the Supplementary material. The experimental results fit well with the simulation. A deterioration of the measured results compared to the simulation can be attributed to the fabrication error.

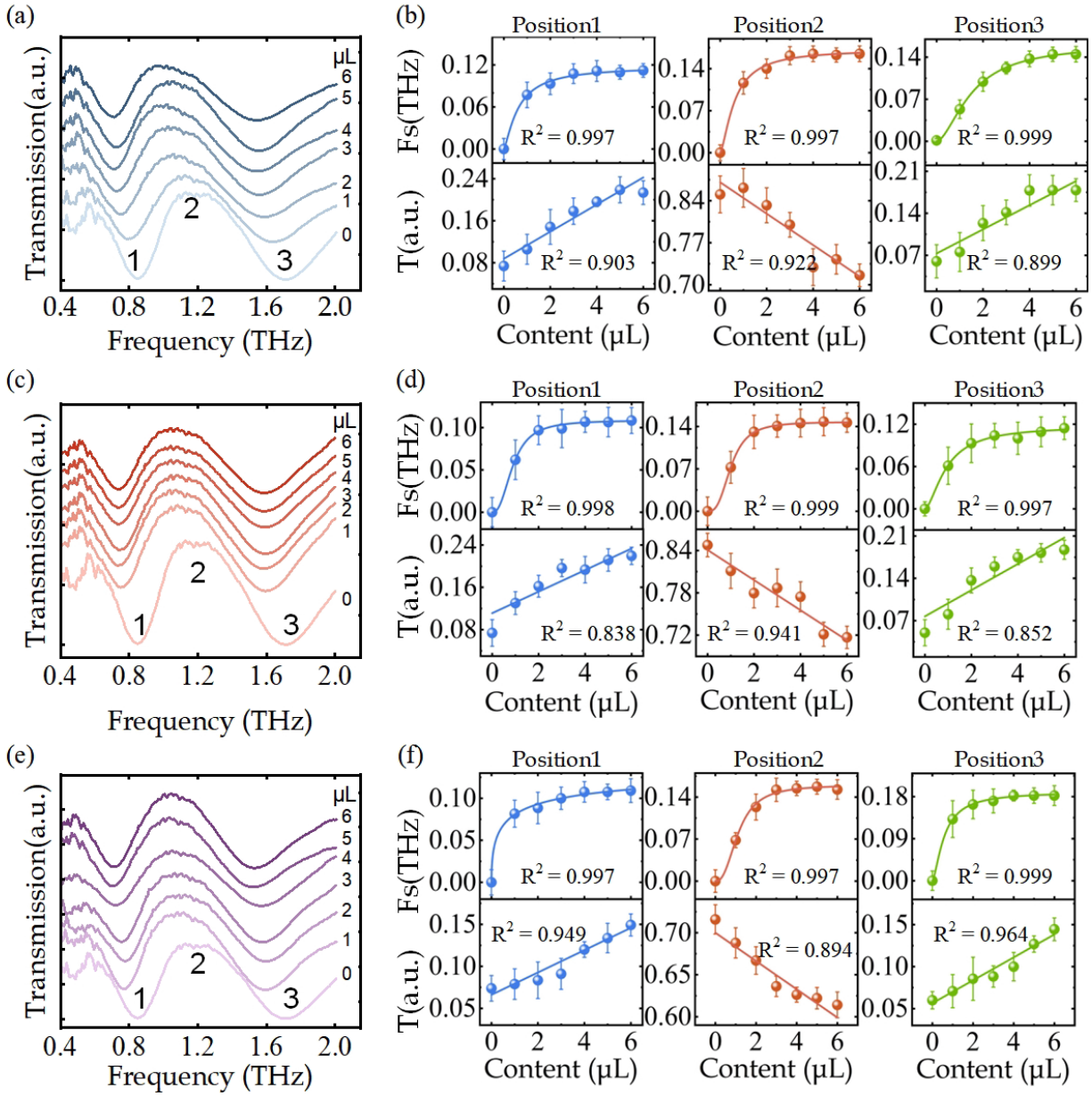

Fig. 4. Experimental results of the transmission spectra, frequency shift response with Hill fitting, and amplitude response with linear fitting corresponding to different volumes used for the detection of (a) and (b) IPA, (c) and (d) EA, and (e) and (f) EB.

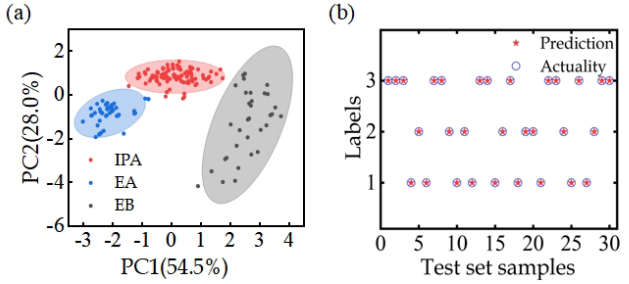

Fig. 5. Classification results for IPA, EA, and EB. (a) PCA-GMM. (b) SVM.

B. Two Classification Based on Multivariate Resonant Response With EIT Meta-Sensors

Principal component analysis (PCA) is well known as a low-dimensional representation to capture more useful information with less features as much as possible. The extracted features, named principal components (PCs), are composed of linearly uncorrelated variables by eliminating the overlapping parts of possibly correlated variables and are ordered with their scores [42], [43]. The scores of PCs mean their maximum variance and their contribution to classification. When the sum of the former PCs is beyond 80%, the former PCs can approximately show all useful information. Moreover, the Gaussian mixed model (GMM) iteratively converges the likelihood function of Gaussian distribution in the model and determines the probability size of a certain point belonging to a certain class for clustering. A regular GMM applies the expectation maximization (EM) algorithm to fit the Gaussian to the dataset and can be used to assure the clusters are distinct in PCA. The PCA-GMM approach can be summarized as feature extraction with PCA and parameter estimation with GMM [44]. In this way, the variance of the GMM

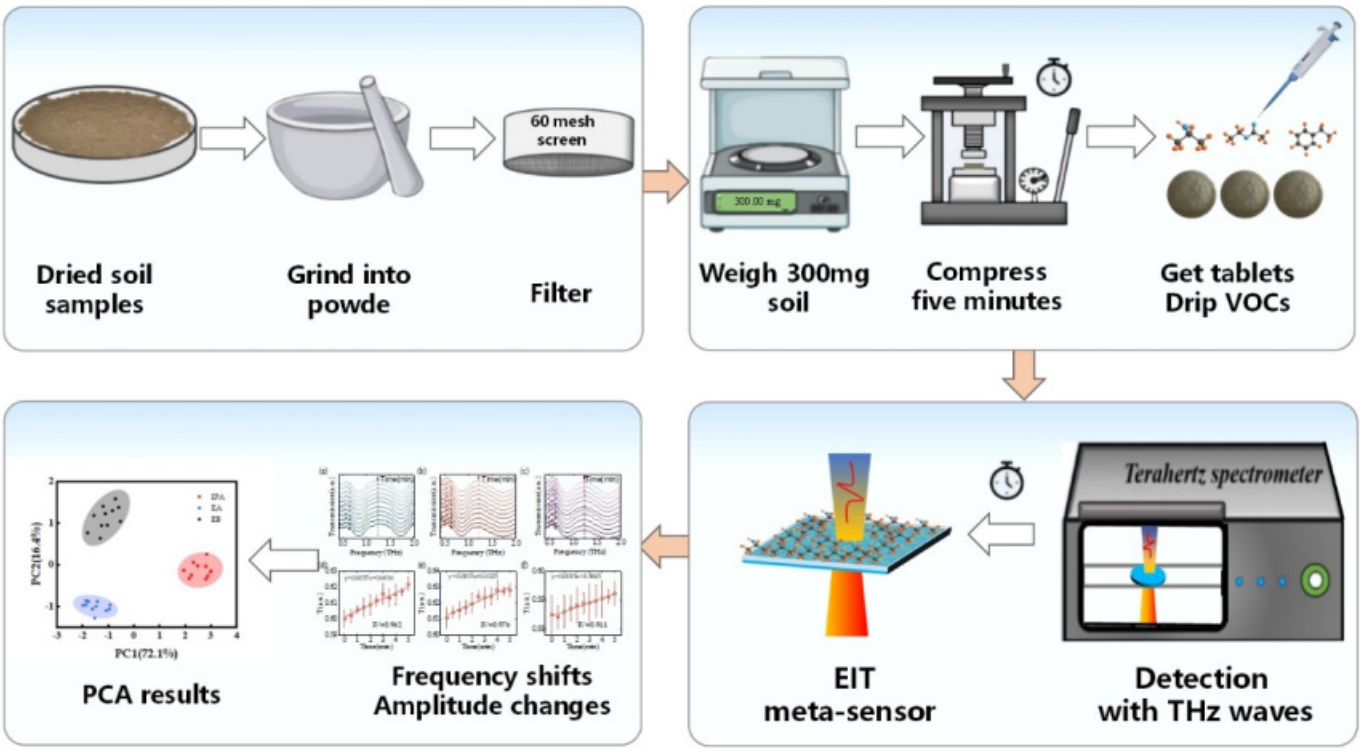

Fig. 6. Diagram of sample preparation, detection, and analyses.

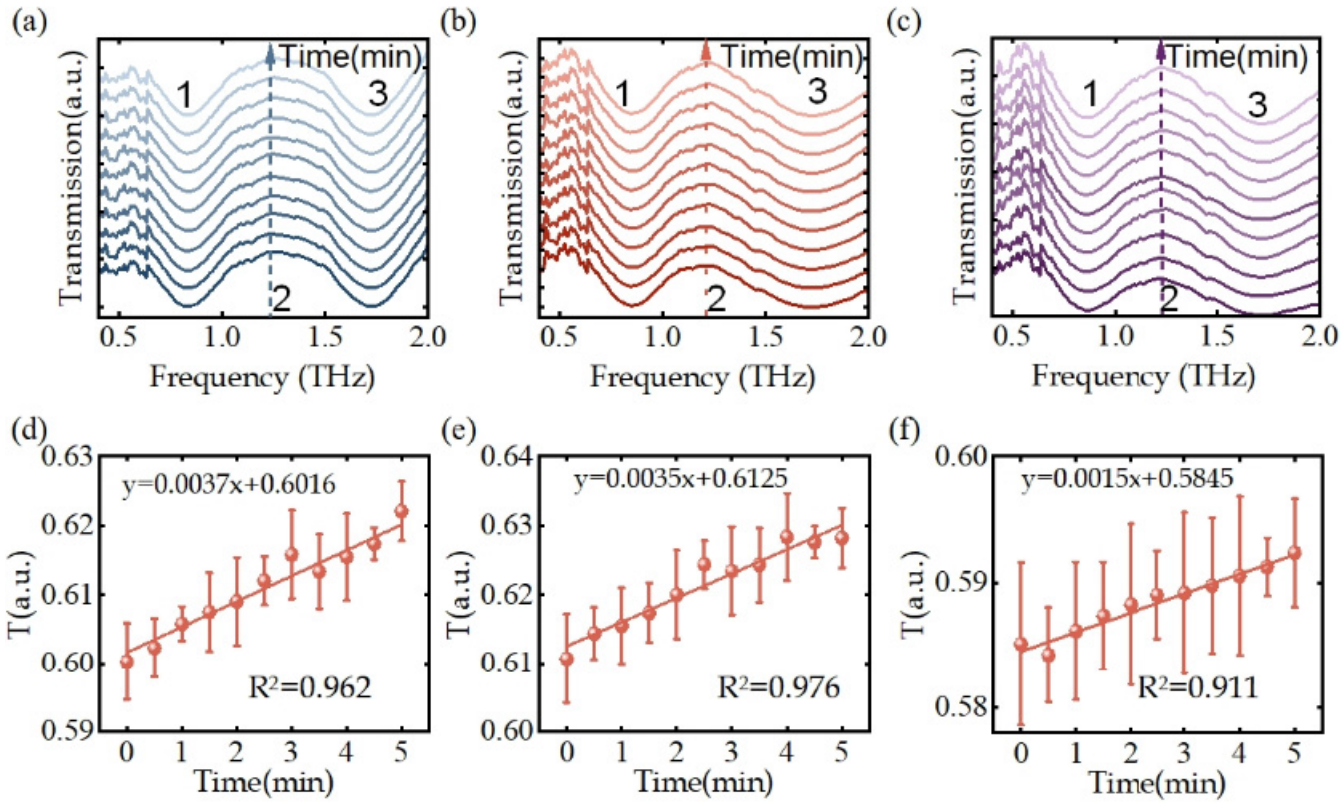

Fig. 7. Univariate fitting results. (a)–(c) THz frequency-domain spectra. (d)–(f) Amplitude response at position 2 with linear fitting when putting VOCs-containing soil tablet on the meta-surface chip with time increasing by 0.5 min, respectively.

can be the additional constraint to confirm the clusters are oval.

In the PCA-GMM algorithm, we substitute the six main parameters of THz EIT spectral data of IPA, EA, and EB with different volumes into the algorithm for calculation. To achieve a more accurate classification, for each VOC with each volume, we measured ten times and obtained 180 sets of data (there were VOCs with six volumes, repeated by ten times). Each set of data includes six EIT parameters (frequencies and intensities of two dips and one peak). The

results are shown in Fig. 5(a). Initial two PCs (PC1 and PC2) were extracted from the dataset and their account in total is 82.5%. Three VOCs were divided into three regions without overlapping each other in brief. However, the distances between IPA and the left two VOCs are close because PC1 is not large enough to fully separate three VOCs. Overall, we can distinguish the three VOCs from each other by PCA-GMM clearly. The SVM classification model, which is suitable for the classification of small samples, is used to classify the VOCs accurately by using the features of the transmission spectrum. The core of the model-building process is the optimal hyperplane whose distance from the different kinds of samples is the maximum [42], [45], [46]. The radial basis function (RBF) [40] as the kernel function aims to make the training procedure complexity lower and reduce the training time. In this work, the SVM classification model is established by using 180 sets of data, each set includes six EIT responses (dual dips and one peak frequency shifts amplitudes changes). The data of each sample are randomly divided into two groups: the training sets group (150) and the test sets group (30). The training set is used to evaluate the accuracy of the model established by the calibration set, and the test set is classified and tested using the trained model. When the model is established by training sets, it can be used to classify the test sets. As shown in Fig. 5(b), the numbers on the y-axis are the class of VOCs (1 represents IPA, 2 represents EA, and 3 represents EB) and the numbers on the x-axis are the order of test set samples. All 30 samples of pure VOCs are predicted correctly into their own class and the accuracy is up to 100%, which proves that it is available to classify pure VOCs with the features extracted from the response of EIT meta-sensors.

C. VOC Classification in Soil Based on EIT MF and PCA

The complex three-phase coexistence system of soil and the adsorption of VOCs lead to more concealment and cannot be detected in time. Therefore, the rapid detection method of VOCs deserves more attention. The preparation, detection, and analysis progress of VOCs-containing soil samples were displayed in Fig. 6. At first, the soil without pollutants was provided by the Shanghai Academy of Environmental Sciences. Then, we baked it at 100 °C in the drying box (Boxun BG2-30) for 2 h to kill the microorganisms and evaporate the water in the soil. Then, the required soil was filtered with 60 mesh screens after grounding the dried soil into power and 300 mg soil was randomly taken to compress under pressure of 1000 T for 5 min to get a 0.5-mm-thick tablet. Next, we dripped 1 μL IPA, EA, and EB on the tablet, which can decrease scatter effects induced by variations in the density of soil powder [47]. We put the VOCs-containing soil tablets on the EIT meta-sensors and detected it with a THz spectrometer every half minute for 5 min. Finally, we analyzed the transmission spectra with PCA-GMM. The detection result in detail and general analysis can be seen in Fig. 6.

As shown in Fig. 7(a)–(c), when the IPA, EA, and EB were dripped into the soil, the frequency shifts of position 1–position 3 are all less than the resolution of the system (1.9 GHz) with increased time. The possible reason for the slight frequency shift may be because only few content of VOCs at the bottom of the soil changes as it is directly in contact with the surface enhancement of the chip. Besides,

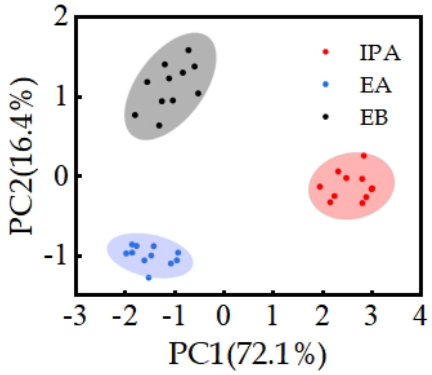

Fig. 8. PCA analysis of dripping IPA, EA, and EB in soil.

the amplitudes from position 1 to position 3 changed with increased time. To show this feature quantitatively, the amplitude variation of position 2 is shown in Fig. 7(d)–(f). It is obvious to find as follows.

1) The amplitude increases linearly with time, indicating that the volatilization of VOCs is linear with increased time. The volatilization of ethanol in the air is about 0.8 μL/min [43], but the volatilization speed of VOCs in the soil is much slower. The soil [44] characterized by the spatial arrangement of solids and voids hinders VOCs from volatilization.

2) After 5 min, the amplitude changes by approximately 0.02 and conforms with the pure VOCs with the same content. That is to say, there are few VOCs left and the limit of VOCs in soil detection is 2600, 3000, and 2900 mg/kg.

3) The amplitude changes of the EIT transmission window are affected in two aspects. On the one hand, the EIT of meta-sensors responds to the changes of VOCs in soil. On the other hand, THz interacts directly with VOCs in soil and the transmission amplitude is changeable with the content of VOCs. Fig. 8 displays the dataset of summarized frequency shifts and amplitudes classified with PCA-GMM. We find that the contribution rates of PC1 and PC2 are 72.1% and 16.4%, respectively. The first two PCs can conclude almost 88.5% of the variance and separate three VOCs without cross-gap and far away from each other. The results prove that trace detection of VOCs in the soil can realize the classification rapidly.

IV. Summary

In this work, a meta-sensor structure based on EIT was proposed to detect VOCs in the microfluidic cell. We focus on the changes of special resonant responses of the EIT meta-sensor (including 0.855, 1.213, and 1.724 THz). For pure IPA, EA, and EB in the liquid phase, when their contents were increased (1–6 μL at intervals of 1 μL), the frequency shifts decreased (red-shift) and satisfy the Hill model, and the frequency and amplitudes satisfied linear fitting. These features can compose the MF framework. Then, the typical classification algorithms PCA-GMM and SVM are used to differentiate pure IPA, EA, and EB by using six resonance features. The accuracy can reach 100%. Finally, VOCs-containing soil was detected by the EIT meta-sensor. Although the volatilization speed of VOCs in the soil is hindered by soil structure and the changes of resonant responses are restricted by VOCs content, the MF with PCA-GMM is still useful

to realize the classification of three VOCs in soil. With the LOD 2900 mg/kg, our results provide a new THz meta-sensor platform to trace the detection of VOCs in the liquid phase and soil, especially in the illegal dumping of hazardous wastes. To further reduce the LOD, some aspects need to be improved: 1) design a new meta-sensor structure that has higher Q and sensitivity, for instance, the bound state in the continuum (BIC) [50]; 2) using the THz system with higher frequency resolution, such as a THz coherent photo-mixing spectrometer setup with 350-MHz resolution [51]; and 3) design special channels to prevent rapid evaporation of trace VOCs.

Acknowledgment

Wenfeng Fu, Hongyan Cao, Shengyuan Shen, Yiming Zhu, and Songlin Zhuang are with the Terahertz Technology Innovation Research Institute, Terahertz Spectrum and Imaging Technology Cooperative, Innovation Center Shanghai Key Laboratory of Modern Optical Systems, University of Shanghai for Science and Technology, Shanghai 200093, China.

Li Sun and Ming Zhou are with the Shanghai Academy of Environmental Sciences, Shanghai 200233, China, and also with the College of Environmental Science and Engineering, Tongji University, Shanghai 200092, China.

Lin Chen is with the Terahertz Technology Innovation Research Institute, Terahertz Spectrum and Imaging Technology Cooperative, Innovation Center Shanghai Key Laboratory of Modern Optical Systems, University of Shanghai for Science and Technology, Shanghai 200093, China, and also with the Shanghai Institute of Intelligent Science and Technology, Tongji University, Shanghai 200092, China (e-mail: linchen@usst.edu.cn).

References

[1] C.-H. Li, "Analysis on the treatment of VOC pollution hazards," in *Proc. IOP Conf. Earth Environ. Sci.*, vol. 791, Jun. 2021, pp. 012201–012206, doi: 10.1088/1755-1315/791/1/012201.

[2] V. Galstyan, A. D'Arco, M. Di Fabrizio, N. Poli, S. Lupi, and E. Comini, "Detection of volatile organic compounds: From chemical gas sensors to terahertz spectroscopy," *Rev. Anal. Chem.*, vol. 40, no. 1, pp. 33–57, Jan. 2021, doi: 10.1515/revac-2021-0127.

[3] H. Wang et al., "Characterization and assessment of volatile organic compounds (VOCs) emissions from typical industries," *Chin. Sci. Bull.*, vol. 58, no. 7, pp. 724–730, Mar. 2013, doi: 10.1007/s11434-012-5345-2.

[4] A. K. Pathak and C. Viphavakit, "A review on all-optical fiber-based VOC sensors: Heading towards the development of promising technology," *Sens. Actuators A, Phys.*, vol. 338, May 2022, Art. no. 113455, doi: 10.1016/j.sna.2022.113455.

[5] M.-C. Reinnig, L. Müller, J. Warnke, and T. Hoffmann, "Characterization of selected organic compound classes in secondary organic aerosol from biogenic VOCs by HPLC/MS n," *Anal. Bioanal. Chem.*, vol. 391, no. 1, pp. 171–182, May 2008, doi: 10.1007/s00216-008-1964-5.

[6] L. Kohl et al., "Technical note: Interferences of volatile organic compounds (VOCs) on methane concentration measurements," *Biogeosciences*, vol. 16, no. 17, pp. 3319–3332, Sep. 2019, doi: 10.5194/bg-16-3319-2019.

[7] G. P. Mishra, D. Kumar, V. S. Chaudhary, and S. Kumar, "Design and sensitivity improvement of microstructured-core photonic crystal fiber based sensor for methane and hydrogen fluoride detection," *IEEE Sensors J.*, vol. 22, no. 2, pp. 1265–1272, Jan. 2022, doi: 10.1109/JSEN.2021.3131694.

[8] V. S. Chaudhary, D. Kumar, and S. Kumar, "SPR-assisted photonic crystal fiber-based dual-wavelength single polarizing filter with improved performance," *IEEE Trans. Plasma Sci.*, vol. 49, no. 12, pp. 3803–3810, Dec. 2021, doi: 10.1109/TPS.2021.3126671.

[9] V. S. Chaudhary, D. Kumar, and S. Kumar, "Gold-immobilized photonic crystal fiber-based SPR biosensor for detection of malaria disease in human body," *IEEE Sensors J.*, vol. 21, no. 16, pp. 17800–17807, Aug. 2021, doi: 10.1109/JSEN.2021.3085829.

[10] V. S. Chaudhary, D. Kumar, G. P. Mishra, S. Sharma, and S. Kumar, "Plasmonic biosensor with gold and titanium dioxide immobilized on photonic crystal fiber for blood composition detection," *IEEE Sensors J.*, vol. 22, no. 9, pp. 8474–8481, May 2022, doi: 10.1109/JSEN.2022.3160482.

[11] V. S. Chaudhary, D. Kumar, B. P. Pandey, and S. Kumar, "Advances in photonic crystal fiber-based sensor for detection of physical and biochemical parameters—A review," *IEEE Sensors J.*, vol. 23, no. 2, pp. 1012–1023, Jan. 2023, doi: 10.1109/JSEN.2022.3222969.

[12] M. Tonouchi, "Cutting-edge terahertz technology," *Nature Photon.*, vol. 1, pp. 97–105, Feb. 2007, doi: 10.1038/nphoton.2007.3.

[13] L. Chen, D.-G. Liao, X.-G. Guo, J.-Y. Zhao, Y.-M. Zhu, and S.-L. Zhuang, "Terahertz time-domain spectroscopy and micro-cavity components for probing samples: A review," *Frontiers Inf. Technol. Electron. Eng.*, vol. 20, no. 5, pp. 591–607, May 2019, doi: 10.1631/FITEE.1800633.

[14] H. J. Shin, S.-W. Choi, and G. Ok, "Qualitative identification of food materials by complex refractive index mapping in the terahertz range," *Food Chem.*, vol. 245, pp. 282–288, Apr. 2018, doi: 10.1016/j.foodchem.2017.10.056.

[15] W.-Z. Luo, Z.-W. Zhang, H.-S. Liu, and C.-L. Zhang, "Terahertz reflection time-domain spectroscopy for measuring alcohol concentration," *Proc. SPIE*, 2018, pp. 202–208.

[16] O. A. Smolyanskaya et al., "Terahertz biophotonics as a tool for studies of dielectric and spectral properties of biological tissues and liquids," *Prog. Quantum Electron.*, vol. 62, pp. 1–77, Nov. 2018, doi: 10.1016/j.pquantelec.2018.10.001.

[17] H. Guerboukha, K. Nallappan, and M. Skorobogatiy, "Toward real-time terahertz imaging," *Adv. Opt. Photon.*, vol. 10, no. 4, pp. 843–938, Dec. 2018, doi: 10.1364/AOP.10.000843.

[18] I. F. Akyildiz, J. M. Jornet, and C. Han, "Terahertz band: Next frontier for wireless communications," *Phys. Commun.*, vol. 12, pp. 16–32, Sep. 2014, doi: 10.1016/j.phycom.2014.01.006.

[19] A. D'Arco et al., "Characterization of volatile organic compounds (VOCs) in their liquid-phase by terahertz time-domain spectroscopy," *Biomed. Opt. Exp.*, vol. 11, no. 1, pp. 1–7, 2020, doi: 10.1364/BOE.11.000001.

[20] D. F. Plusquellic, K. Siegrist, E. J. Heilweil, and O. Esenturk, "Applications of terahertz spectroscopy in biosystems," *Chem. Phys. Chem.*, vol. 8, no. 17, pp. 2412–2431, 2007, doi: 10.1002/cphc.200700332.

[21] R. B. Barnes, W. S. Benedict, and C. M. Lewis, "The far infrared absorption of benzene," *Phys. Rev.*, vol. 47, no. 2, pp. 129–130, Jan. 1935, doi: 10.1103/PhysRev.47.129.

[22] C. Ro/nne, K. Jensby, B. J. Loughnane, J. Fourkas, O. F. Nielsen, and S. R. Keiding, "Temperature dependence of the dielectric function of C_6H_6(l) and $C_6H_5CH_3$(l) measured with THz spectroscopy," *J. Chem. Phys.*, vol. 113, no. 9, pp. 3749–3756, Sep. 2000, doi: 10.1063/1.1287737.

[23] T. Ikeda et al., "Investigation of inflammable liquids by terahertz spectroscopy," *Appl. Phys. Lett.*, vol. 87, no. 3, Jul. 2005, Art. no. 034105, doi: 10.1063/1.1999847.

[24] L. Chen et al., "Tunable phase transition via radiative loss controlling in a terahertz attenuated total reflection-based metasurface," *IEEE Trans. Terahertz Sci. Technol.*, vol. 9, no. 6, pp. 643–650, Nov. 2019, doi: 10.1109/TTHZ.2019.2937504.

[25] N. Born, I. Al-Naib, C. Jansen, T. Ozaki, R. Morandotti, and M. Koch, "Excitation of multiple trapped-eigenmodes in terahertz metamolecule lattices," *Appl. Phys. Lett.*, vol. 104, no. 10, Mar. 2014, Art. no. 101107, doi: 10.1063/1.4868420.

[26] H. Tao et al., "Metamaterials on paper as a sensing platform," *Adv. Mater.*, vol. 23, no. 28, pp. 3197–3201, Jul. 2011, doi: 10.1002/adma.201100163.

[27] L. Chen et al., "Defect-induced Fano resonances in corrugated plasmonic metamaterials," *Adv. Opt. Mater.*, vol. 5, no. 8, Apr. 2017, Art. no. 1600960, doi: 10.1002/adom.201600960.

[28] R. Singh, W. Cao, I. Al-Naib, L. Cong, W. Withayachumnankul, and W. Zhang, "Ultrasensitive terahertz sensing with high-Q Fano resonances in metasurfaces," *Appl. Phys. Lett.*, vol. 105, no. 17, Oct. 2014, Art. no. 171101, doi: 10.1063/1.4895595.

[29] P. Nie, D. Zhu, Z. Cui, F. Qu, L. Lin, and Y. Wang, "Sensitive detection of chlorpyrifos pesticide using an all-dielectric broadband terahertz metamaterial absorber," *Sens. Actuators B, Chem.*, vol. 307, Mar. 2020, Art. no. 127642, doi: 10.1016/j.snb.2019.127642.

[30] J.-Q. Zhang et al., "Optimized bow-tie metasurface and its application in trace detection of lead ion," *Opto-Electron. Eng.*, vol. 48, no. 8, pp. 59–68, 2021, doi: 10.12086/OEE.2021.210123.

[31] F. Qu, L. Lin, Z. Chen, A. Abdalla, and P. Nie, "A terahertz multi-band metamaterial absorber and its synthetic evaluation method based on multivariate resonant response fusion for trace pesticide detection," *Sens. Actuators B, Chem.*, vol. 336, Jun. 2021, Art. no. 129726, doi: 10.1016/j.snb.2021.129726.

[32] L. Liang et al., "Unity integration of grating slot waveguide and microfluid for terahertz sensing," *Laser Photon. Rev.*, vol. 12, no. 11, Nov. 2018, Art. no. 1800078, doi: 10.1002/lpor.201800078.
[33] L. Chen et al., "Mode splitting transmission effect of surface wave excitation through a metal hole array," *Light, Sci. Appl.*, vol. 2, no. 3, p. e60, Mar. 2013, doi: 10.1038/lsa.2013.16.
[34] L. Wang et al., "Enhanced THz EIT resonance based on the coupled electric field dropping effect within the undulated metasurface," *Nanophotonics*, vol. 8, no. 6, pp. 1071–1078, Jun. 2019, doi: 10.1515/nanoph-2019-0040.
[35] L. Zhu et al., "Polarization conversion based on Mie-type electromagnetically induced transparency (EIT) effect in all-dielectric metasurface," *Plasmonics*, vol. 13, no. 6, pp. 1971–1976, Dec. 2018, doi: 10.1007/s11468-018-0712-8.
[36] Y.-S. Lin et al., "Soil enviromental quality risk control standard for soil contamination of agricultural land," Nanjing Inst. Environ. Sci., Ministry Ecol. Environ., Jiangsu, China, Tech. Rep. GB 15618-2018, 2018.
[37] X.-J. Xiao, Y. Wang, X. Zhang, T. Zhou, K, Zhang. X. Wang, "Carbon nanotubes film integrated with silicon microfluidic channel for a novel composite THz metasurface," *IEEE J. Sel. Topics Quantum Electron.*, vol. 28, no. 3, Oct. 2022, Art. no. 8500108, doi: 10.1109/JSTQE.2021.3116969.
[38] N. Pandit, R. K. Jaiswal, and N. P. Pathak, "Towards development of a non–intrusive and label–free THz sensor for rapid detection of aqueous bio–samples using microfluidic approach," *IEEE Trans. Biomed. Circuits Syst.*, vol. 15, no. 1, pp. 91–101, Feb. 2021, doi: 10.1109/TBCAS.2021.3050844.
[39] J. Xu et al., "Terahertz microfluidic sensing with dual-torus toroidal metasurfaces," *Adv. Opt. Mater.*, vol. 9, no. 15, Aug. 2021, Art. no. 2100024, doi: 10.1002/adom.202100024.
[40] X. Yan, M. Yang, Z. Zhang, T. W. Wei, L. Liu, and J. Xie, "The terahertz electromagnetically induced transparency-like metamaterials for sensitive biosensors in the detection of cancer cells," *Biosensors Bioelectron.*, vol. 126, pp. 485–492, Feb. 2019, doi: 10.1016/j.bios.2018.11.014.
[41] R.-Q. Yan et al., "Highly sensitive plasmonic nanorod hyperbolic metamaterial biosensor," *Photon. Res.*, vol. 10, no. 1, pp. 84–95, Jan. 2022, doi: 10.1364/PRJ.444490.
[42] T. Chen et al., "Classification and recognition of genetically modified organisms by chemometrics methods using terahertz spectroscopy," *Int. J. Food Sci. Technol.*, vol. 50, no. 12, pp. 2682–2687, Dec. 2015, doi: 10.1111/ijfs.12942.
[43] Z. Wang et al., "Qualitative and quantitative recognition of chiral drugs based on terahertz spectroscopy," *Analyst*, vol. 146, no. 12, pp. 3888–3898, Jun. 2021, doi: 10.1039/d1an00500f.
[44] L. Jiang, B. Zhu, H. Jing, X. Chen, X. Rao, and Y. Tao, "Gaussian mixture model-based walnut shell and meat classification in hyperspectral fluorescence imagery," *Trans. ASABE*, vol. 50, no. 1, pp. 153–160, 2007.
[45] S. Yang et al., "Determination of the geographical origin of coffee beans using terahertz spectroscopy combined with machine learning methods," *Frontiers Nutrition*, vol. 8, Jun. 2021, doi: 10.3389/fnut.2021.680627.
[46] X. Wang, K.-X. Hu, L. Zhang, X. Yu, and E.-J. Ding, "Characterization and classification of coals and rocks using terahertz time-domain spectroscopy," *J. Infr., Millim., Terahertz Waves*, vol. 38, no. 2, pp. 248–260, Feb. 2017, doi: 10.1007/s10762-016-0317-2.
[47] S. Zhao, Y. Zhang, Z. Qiu, Y. He, and Y. Zhang, "Towards a fast and generalized microplastic quantification method in soil using terahertz spectroscopy," *Sci. Total Environ.*, vol. 841, Oct. 2022, Art. no. 156624, doi: 10.1016/j.scitotenv.2022.156624.
[48] S.-P. Huang, C.-G. Xue, Y.-S. Mei, and Y.-L. HU, "Application of microcantilever sensor system in ethanol volatilization detection," *Transducer Microsyst. Technol.*, vol. 39, no. 8, pp. 158–160, 2020, doi: 10.13873/J.1000-9787(2020)08-0158-03.
[49] E. Rabot, M. Wiesmeier, S. Schlüter, and H.-J. Vogel, "Soil structure as an indicator of soil functions: A review," *Geoderma*, vol. 314, pp. 122–137, Mar. 2018, doi: 10.1016/j.geoderma.2017.11.009.
[50] Y. K. Srivastava, R. T. Ako, M. Gupta, M. Bhaskaran, S. Sriram, and R. Singh, "Terahertz sensing of 7 nm dielectric film with bound states in the continuum metasurfaces," *Appl. Phys. Lett.*, vol. 115, no. 15, Oct. 2019, Art. no. 151105.
[51] M. Zhang et al., "Terahertz spectroscopic signatures of microcystin aptamer solution probed with a microfluidic chip," *Sensors*, vol. 19, no. 3, p. 534, Jan. 2019, doi: 10.3390/s19030534.

Wenfeng Fu received the B.S. degree in electronic information science and technology from the University of Shanghai for Science and Technology, Shanghai, China, in 2020, where she is pursuing the M.S. degree in information and communication engineering.

Her research interests include terahertz bioassay.

Li Sun received the B.S. degree in chemical engineering and technology from the Harbin Institute of Technology, Harbin, China, in 2008, and the M.S. degree in environmental science from Nanjing University, Nanjing, China, in 2011. She is currently pursuing the Ph.D. degree in environmental engineering with Tongji University, Shanghai, China.

Since 2011, she has been working with the Shanghai Academy of Environmental Sciences, Shanghai. Her research interests include terahertz spectrum detection, solid waste management, clean production, and carbon emission reduction. She has presided over more than ten scientific research projects from the Shanghai Science and Technology Commission and the Shanghai Municipal Bureau of Ecological Environment. She also has managed more than 50 research projects from district governments, industrial parks, and enterprises.

Hongyan Cao received the B.S. degree in electronic information science and technology from Huaiyin Normal University, Huaian, China, in 2020. She is pursuing the M.S. degree in information and communication engineering with the University of Shanghai for Science and Technology, Shanghai, China.

Her research interests include terahertz bioassay.

Lin Chen (Member, IEEE) received the B.S. and M.S. degrees in electrical engineering from Southeast University, Jiangsu, China, in 2002 and 2005, respectively, and the Ph.D. degree in optics from Shanghai Jiao Tong University, Shanghai, China, in 2008.

From 2007 to 2008, he was with Avanex Corporation, Fremont, CA, USA, as a Senior Engineer. From 2012 to 2013, he was a Visiting Scholar with the State Key Laboratory of Millimeter Waves, Southeast University. From 2015 to 2016, he was a Visiting Researcher with the Ultrafast THz Optoelectronic Laboratory, Oklahoma State University, Stillwater, OK, USA. At present, he has published more than 70 peer-reviewed papers with more than 2000 citations and an H-index of 26 (including four highly cited papers) in Science Citation Indexed journals such as *Light: Science & Applications*. He has also applied for more than 40 invention patents, 21 authorized and one U.S. patent.

Dr. Chen was designated Shanghai "Dawn Scholar," "Chengguang Scholar," "Top-Notch Young Talents," "Rising-Star," "Pujiang Talent," and other talent titles. He received the Publons Peer Review Award (2018 and 2019). As the first person in charge, he has undertaken a number of national-level projects, including the National Key Research and Development Plan "Major Scientific Instrument And Equipment Development" (Chief Scientist), two National Major Instrument Projects (project), the National Natural Foundation of China (General and Youth), and several projects in Shanghai. He is currently the Editorial Board Member of *Frontiers in Physics* and a Guest Editor and the Corresponding Expert of *Frontiers of Information Technology & Electronic Engineering*.

Ming Zhou was born in Shanghai, China, in July 1971. He received the bachelor's degree in biochemistry from Huaqiao University, Quanzhou, Fujian, China, in 1993.

In 1993, he joined the Shanghai Academy of Environmental Sciences, Shanghai, and engaged in environmental impact assessment. In 1997, he joined the Institute of Solid Waste Pollution Prevention and Control Technology and engaged in cleaner production, solid waste pollution prevention and control, and environmental management system certification. In 2009, he served as the Director of the Clean Production and Environmental Audit Center and the General Manager of Shanghai Huanke Environmental Certification Company Ltd. In 2016, he was engaged in the planning of eco-industrial parks, carried out scientific research on solid waste and hazardous waste for the Shanghai Municipal Bureau of Ecological Environment, undertook and participated in more than 20 scientific research projects of the Shanghai Municipal Bureau of Ecological Environment, understood the relevant technical requirements of Shanghai's hazardous waste management, and has published several theoretical papers and monographs on environmental management. In 2019, he jointly established the Terahertz Technology Innovation and Application Joint Laboratory, Shanghai University of Technology, Shanghai, to carry out research on the application of terahertz technology in the field of environment, especially in the detection of hazardous waste, chemicals, and persistent organic pollutants. In 2023, he served as the Director of the Solid Waste Recycling Branch of the Shanghai Environmental Science Society.

Dr. Zhu won the Title of "New Century Talent" from the Ministry of Education in 2012. In 2013, he was appointed as a Council Member of the China Instrument and Control Society. In 2014, he won the title of "Excellent Academic Leaders of Shanghai," and was appointed as a Council Member of the China Optical Engineering Society and a member of the China Youth Scientist and Technician Association. In 2016, he was selected as a "Shanghai Leading Talent" and a "Young Yangtze Scholar." In 2017, he was awarded the "Outstanding Youth Foundation" by the "National Natural Science Foundation of China," and selected for "The National Key Talent Project." In 2018, he was recognized as a "Youth Science and Technology Innovation Leader" by the "Ministry of Science and Technology of China," and received a special State Council allowance. Furthermore, he also won the First Prize in the Shanghai Teaching Achievement Award. He is currently the Director of the Terahertz Spectral and Imaging Technology National Cooperative Innovation Center, the Terahertz Precision Biomedical Technology Overseas Expertise Introduction Center for Discipline Innovation, and the Terahertz Technology Innovation International Joint Laboratory at the University of Shanghai for Science and Technology and Lomonosov Moscow State University.

Shengyuan Shen received the B.S. degree in applied physics from Yanshan University, Hebei, China, in 2020. He is currently pursuing the M.S. degree in optical engineering with the University of Shanghai for Science and Technology, Shanghai, China.

Yiming Zhu (Senior Member, IEEE) received the Ph.D. degree from the University of Tokyo, Tokyo, Japan, in 2008.

He is a "Youth Science and Technology Innovation Leader" and a "Young Yangtze Professor" with the University of Shanghai for Science and Technology, Shanghai, China, and currently serves as the Vice Director of the Shanghai Key Laboratory of Modern Optical Systems. He is also the "National Key Talent Project," the "Outstanding Youth Foundation," and the "Special State Council Allowance" Winner. Up to now, he has published more than 100 papers, including $>$40 papers in *Light: Science & Applications*, *Advanced Optical Materials*, *Applied Physics Letters*, *Optics Letters*, and *Optics Express* (top 5%), including five papers selected as ESI papers. He has been responsible for more than 20 projects at the national and ministerial/provincial levels, which include one project supported by the National 863 Project, four projects supported by the National Natural Science Foundation of China, two subprojects supported by the National 973 Project, and two projects supported by the Major National Development Project of Scientific Instrument and Equipment. His research interests include terahertz technologies and applications, including terahertz devices, terahertz spectroscopy, imaging systems, and terahertz bioapplications.

Songlin Zhuang received the B.S. degree from the Physics Department, Fudan University, Shanghai, China, in 1962, and the Ph.D. degree from the Department of Electronic Engineering, Pennsylvania State University, State College, PA, USA, in 1982.

From 1962 to 1979, he worked at the Shanghai Institute of Optical Instruments, Shanghai. In 1979, he went to Michigan State University, East Lansing, MI, USA, for visiting research. In 1983, he returned to the Shanghai Institute of Optical Instruments as the Director and a Senior Engineer. From 1988 to 1992, he served as the Director and a Researcher with the Shanghai Institute of Laser Technology, Shanghai. Since 1995, he has been the President of the School of Optical-Electronic and Computer Engineering, University of Shanghai for Science and Technology, Shanghai. He has won many ministerial-level science and technology progress awards and many honorary awards. He has designed more than a hundred kinds of optical systems and instruments. He is the first researcher to carry out optical system CAD in China. He presided over and completed the largest optical instrument design software system in China and made original achievements in the optimization method of statistical test total extreme value and the nonlinear model of tolerance. In the field of optical image psychophysics experiments, he carried out the first work in China. He has made comprehensive and systematic research on incoherent optical information processing and rainbow holography and is known as "one of the main contributors of modern white light information processing." A variety of optical methods have been proposed in the study of phase recovery of complex objects, which has opened up a new research direction in this field. The CdSe liquid crystal light valve reached the international advanced level at that time. His outstanding achievements have been made in super-resolution optical imaging, grating diffraction vector mode theory, high-speed optical multichannel mode/number transformation, transformation optics, and artificial medium materials. Over the years, he has personally supervised more than 20 master's and doctoral students. The graduates have made a lot of contributions in the field of optical engineering at home and abroad. One of his students' doctoral dissertation was selected as the National 100 Excellent Doctoral Dissertations in 2009. The course of optical information technology that he taught won the National Excellent Course in 2008.